

## REVERSE BULGING AND PLUGGING IN METAL FOIL INDUCED BY HIGH POWER LASER

Y. C. Zhou<sup>1,2</sup>, Z. P. Duan<sup>2</sup>

<sup>1</sup>Institute of Fundamental Mechanics and Material Engineering, Xiangtan University, Xiangtan, Hunan, 411105, China

<sup>2</sup>Institute of Mechanics, CAS, Beijing, 100080, P. R. China

### ABSTRACT

A new failure mode is observed in circular brass foils induced by laser beam. The new failure is based on the following experimental facts: (1) the peripheries of the circular brass foils are fixed and the surfaces of the foils are radiated by a laser beam; (2) the laser beam used is considered to be non-Gaussian spatially, actually an approximately uniform distribution limited in a certain size spot; (3) the pulse duration of the laser beam is  $250 \mu\text{s}$ , i.e. so called long duration pulse laser. The failure process consists of three stages; i.e., thermal bulging, localized shear deformation and perforation by plugging. The word 'reverse' in 'reverse bulging and plugging mode' means that bulging and plugging occur in the reverse direction of laser beam incidence. The new failure mode is analyzed with the thermal-elastic plate theory, parabolic shear deformation theory as well as one-dimensional buckling theory. The theoretical study can explain the new phenomenon and predict the critical laser intensity. The calculated results for temperature fields, deflection as well as shear deformation distribution show that the newly discovered failure mode is attributed to the spatial structure effect of laser beam indeed.

### KEYWORDS

High power laser beam, Circular brass foil, Reverse bulging and plugging

### INTRODUCTION

In the last two decades, a great deal of attention had been paid to the interaction of high power laser with material in the fields of materials and/or structural damage and laser processing [1-2]. The damage modes which may be spallation, melting and/or vaporization depend on laser parameters, for example laser power, laser beam diameter and pulse duration. There is the potential of failure by thermal stress for the intensity of CW (continuous wave) laser in the order of  $10^3 \text{ W/cm}^2$ . The damage may occur by melting and/or vaporization for the laser intensity in the order of  $10^5 - 10^8 \text{ W/cm}^2$  and the pulse duration in the order of milliseconds. In this case, the thermal stress concentrated around the crater plays an important role in material and/or structure damage. The formation of plasma may generate shock waves propagating into the materials for the laser intensity in the order of  $10^8 - 10^{10} \text{ W/cm}^2$  and the pulse duration in the order of nanoseconds. When the wave reflection takes place between two surfaces, there is the potential of failure by spallation.

However, people ignored more or less the fact that the spatial shapes of the laser beam could also play an

important role in controlling the failure mode. Those situations prevail where the size and intensity of the laser beam are such that the spatial structure effect will contribute to the mode of failure such as bulging followed by plugging. Such are the cases considered in this investigation.

## EXPERIMENTAL PROCEDURE AND OBSERVATION

### Experimental Procedure

A new kind of failure mode was observed in circular brass foils in which their peripheries were fixed and their front surface was subjected to a long pulsed laser over a central region, as shown in Fig.1(a). In the figure,  $z$ - and  $r$ -direction are aligned normal and parallel to the specimen, respectively,  $2a$  is the diameter of the laser spot with size 2-6mm. The foil has a diameter of 30mm and thickness of 0.1mm and is composed of 65% copper, 33.6% zinc, 0.03% iron, 0.06% antimony and other microelements that are negligibly small in percentage by weight.

The laser beam used is a single pulse Nd: glass with a wavelength of  $1.06\mu\text{m}$ , intensity order of  $10^5$ - $10^6\text{W}/\text{cm}^2$  and energy from 25-40J. The diagnostics of the laser parameters provide a traditional monitoring of the laser beam characteristics, such as energy, temporal and spatial shapes. In the experiment, temperature rise on the rear surface of samples during laser irradiation is measured by a focused, imaging system of infrared (IR) detectors. The particular system consists of eight  $0.1\times 0.1\text{mm}$  indium antimonide (INSb) Infrared detectors mounted on a liquid nitrogen Dewar bottle.

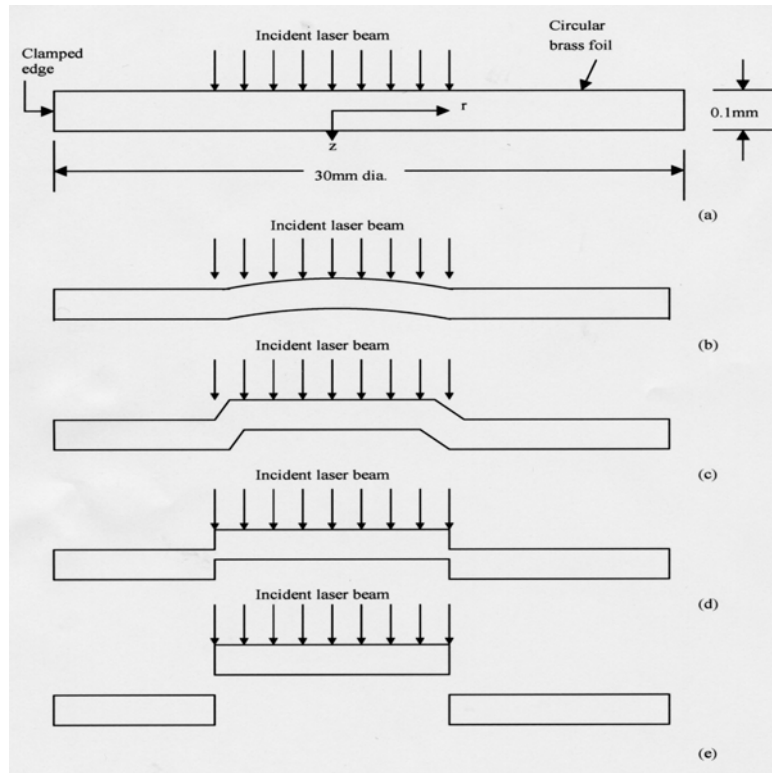


**Figure 1:** Schematics of the sample and failure mode: (a) schematic diagram of a normal incident laser beam impinging on a circular brass foil specimen; (b) bulging; (c) localized shear deformation; (d) plugging initiation; (e) perforation

The normalized laser intensity  $I/I_{\text{max}}$  vs time and space coordinates  $r/a$  is shown in figure 2, where  $r$  and  $a$  are the radial distance and the radius of the laser spot, respectively. The full time width at half maximum of the laser is approximately  $250\mu\text{s}$ . The laser intensity distribution of laser intensity is non-Gaussian and roughly uniform within the laser irradiated region and declines very sharply towards the edge where the laser spot terminates. For the convenience of numerical analysis, the laser intensity  $I$  is approximated by,

$$I = I_{\text{max}} e^{-\alpha t} (1 - e^{-\beta t}) f(r) = I_{\text{max}} g(t) f(r) \quad (1)$$

where  $\alpha$  and  $\beta$  are determined experimentally test, and equal to  $1.5\times 10^4/\text{s}$  and  $8.0\times 10^4/\text{s}$ , respectively. Therefore, laser energy  $E_j = \beta\pi a^2 I_{\text{max}} / \alpha(\alpha + \beta)$  and we have

$$f(r) = \begin{cases} 1 & , \quad 0 \leq r \leq a \\ 0 & , \quad a \leq r \leq \infty \end{cases} \quad (2)$$

and  $f(r) = e^{-(r/a)^2}$  which are characterized by the non-Gaussian and Gaussian nature of the laser beam, respectively.

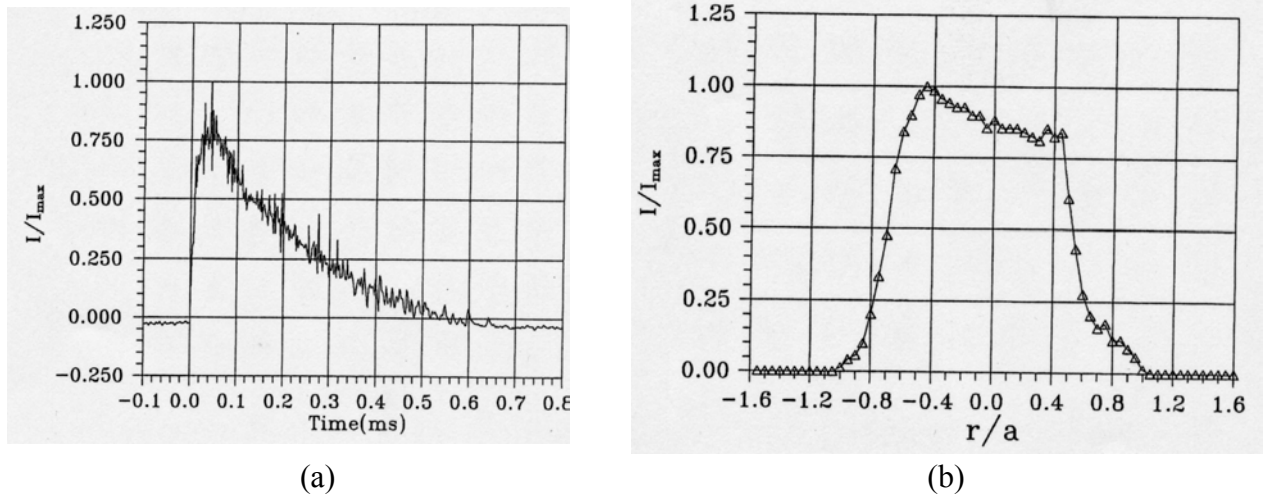


**Figure 2:** Temporal and spatial shape of Nd:glass pulsed laser intensity, (a) temporal shape, (b) spatial shape

### Experimental Results

#### Description of failure mode

The evolution of specimen failure is illustrated schematically in Fig.1. Fig.1(b) shows bulging of the brass foil at the earlier stage of laser irradiation. Note that this occurs towards the side of the incident laser beam where the temperature would be higher. Significant shear deformation occurs around a rim near the outer edge of the laser beam which is shown in Fig.1(c). This leads to the softening of the material due to intense heating.

Further intensification of the energy around the periphery of the laser beam leads to the initiation of plugging and final perforation which are shown in Fig.1(d)-(e), respectively. The plugging mode of failure is customarily known to be associated with metal projectiles penetrating through metal targets in plate form. A plug of the target material is normally ejected in the direction of the energy source that is the moving projectile. While in the present case of laser induced the new failure mode, the plug is normally ejected in the direction opposite to the incident laser beam. The initial bulging occurs on the side with higher temperature that determines the direction of plugging.

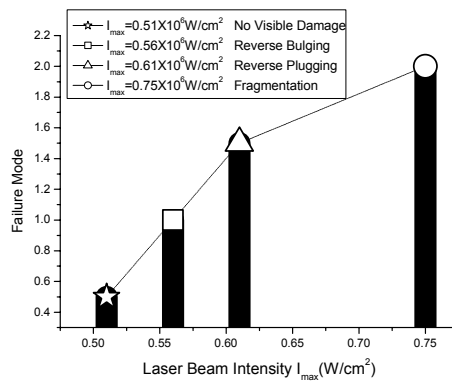


**Figure 3:** Failure mode in brass foil

#### Threshold intensity

According to the test data in this study, the failure modes and their related threshold are shown in figure 3. When the laser energy density was lower than  $151 \text{ J/cm}^2$ , or equivalently, the laser intensity was less than

$0.51 \times 10^6 \text{W/cm}^2$ , no visible macroscopic damage was observed on the front or rear surface of the brass specimen. When the laser intensity was increased to  $0.56 \times 10^6 \text{W/cm}^2$ , the bulging of the brass specimen was observed. A slight melting was observed on the front surface at the periphery of the laser spot. The laser intensity threshold value  $I_{cr}$  for plugging to occur was about  $0.61 \times 10^6 \text{W/cm}^2$ . As  $I$  exceeds  $I_{cr}$ , local melting of the material begins to take place. When the laser intensity was increased to  $0.75 \times 10^6 \text{W/cm}^2$ , the brass foil was totally fractured and fragmented. A study on laser-induced spallation in 0.1mm thickness copper foil has been made by Eliezer and coworkers[2]. The intensity for spallation was of the order of  $5.3 \times 10^{10} \text{W/cm}^2$  which was five orders of magnitude larger than that for that for failure by plugging which was about  $0.71 \times 10^6 \text{W/cm}^2$ . The thresholds of the laser energy for the two different failure modes are almost not distinguishable and they are both approximately equal to  $210 \text{J/cm}^2$ .

### Damage evolution

Scanning electron microscopy (SEM) showed that increased laser intensity led to the initiation of microcracks in the peripheral region with  $r \sim a$ . The macrocracks appeared on the rear surface and then spread into the material. They would grow and coalesce into macrocracks that rapidly in the circumferential direction as well as in the thickness direction. The macroscopic damage evolutions are shown in figures 4(a), (b) and (c) which, respectively, correspond to the schematic illustration of damage evolutions as shown in Fig.1(b), (d) and (e). The photograph of a polished section of brass specimen is shown in figure 4(a). Bulging in the direction opposite to the incident laser beam was observed with a maximum center deflection of 0.03mm which corresponded to a laser energy of 8.2J; an intensity greater than  $0.61 \times 10^6 \text{W/cm}^2$ , and a spot diameter of 2.3mm. Softening of the material began around the outer edge of the laser spot.

When the laser intensity was increased to  $0.61 \times 10^6 \text{W/cm}^2$ , the plugging began to take place in the brass foil. Figure 4(b) shows the circular brass foil failed by plugging opposite to the direction of the incident laser beam. This photograph of brass foil failure by plugging is viewed from the rear surface with a laser energy of 29J over region 4.5mm in diameter and the failure process corresponds to that described in Fig.1 (d).

When the intensity was increased to  $0.75 \times 10^6 \text{W/cm}^2$  the brass foil is totally fractured and fragmented. Figure 4(c) shows a sectioned photograph of fractured and fragmented brass foil subjected to a laser energy of 9.2J over a region 2.3mm in diameter and the failure process corresponds to that described in Fig.1(e).

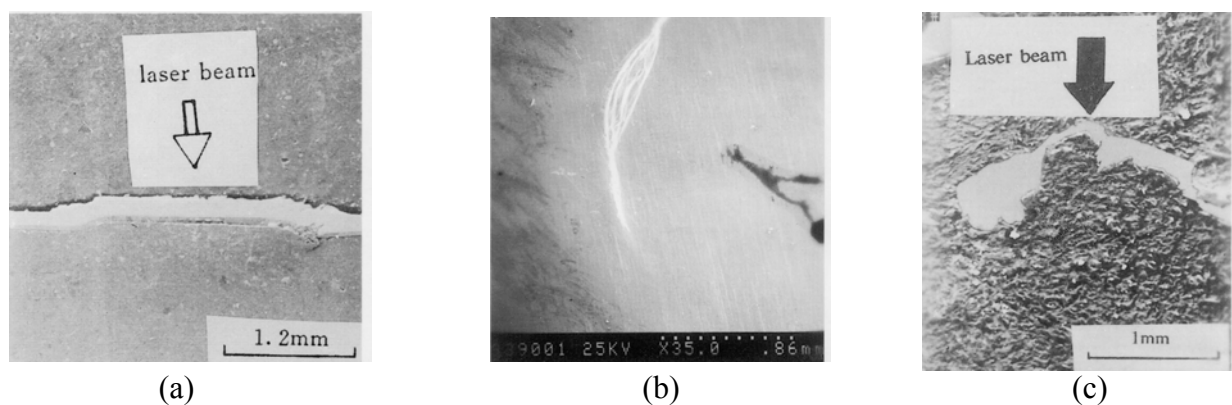


**Figure 4:** Photograph of failure mode: (a) sectioned photograph at the bulging state with a laser energy of 8.2J over an area of 2.3mm in diameter; (b) photograph of failure by plugging viewed from the rear surface with laser energy of 29J over a region 4.5mm in diameter; (c) photograph of fractured and fragmented foil subjected to a laser energy of 9.2J over a region 2.3mm.

## DISCUSSIONS

### A Thermal-elastic Analysis

As shown in section 2, at the earlier stage of laser irradiation, the brass foil bulged towards the side of the incident laser beam. The classical Kirchhoff plate theory can be used to determine the reverse bulging. In the analysis, the temperature distributions are obtained in terms of Hankel transformation and series expansion techniques. Using this temperature solution and classical Kirchhoff plate theory, deflection curve, i.e.,

reverse bulging  $w$  can be determined analytically under the assumption of thermal-mechanical decoupling. Fig.8 shows the three-dimensional profile of deflection curve for the brass foil. The thermal-elastic analysis reveal that: (a) thermal reverse bulging is mainly due to highly non-uniform spatial distribution of temperature in normal direction of target material, i.e., the temperature gradient in  $z$ -direction; (b) a steep temperature gradient across the periphery of the laser spot causes the shear strain at the periphery of the laser spot to be much larger than that in other regions. It is the temperature rise and subsequent shear deformation localization which control the whole process of the new failure mode. (c) The spatial structure of the laser beam plays an important role in controlling the damage.

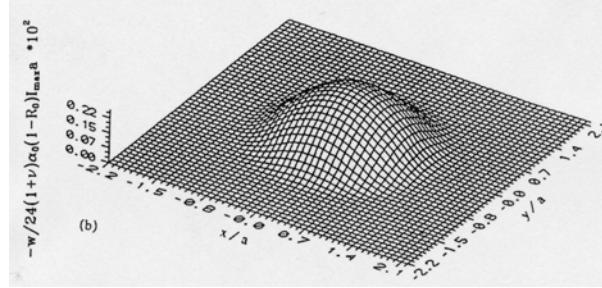


**Figure 5:** Three-dimensional profile of deflection curve for the brass foil.

### *Shear Deformation Analysis*

We obtained new coupled governing equations of shear deformation and large deflections of a heated, non-homogeneous circular plate. The governing equations are obtained based on the large deflections of Berger [1] and the parabolic shear deformation theory of Bhimaraddi and Stevens [1]. We use the new coupled governing equations to analyze the failure mode induced by laser. The new non-linear coupled equations were solved by employing the Galerkin and iterative methods. Numerical results of the average shear strain at different time are shown in Fig.6. It is observed that only the shear strain  $\gamma$  is not zero within the laser spot edge region. This important result confirms the experimental observation, i.e. the existence of large shear strain  $\gamma$  within the laser spot edge. From the comparison of the shear strain distribution induced by a non-Gaussian laser beam and by a Gaussian laser beam, one can conclude that the former offers a formidable potential for the new type of failure by plugging, however, the latter has a little potential for the new type of failure by plugging. This reveals that the spatial shapes of a laser beam, indeed, play an important role in controlling the damage types.

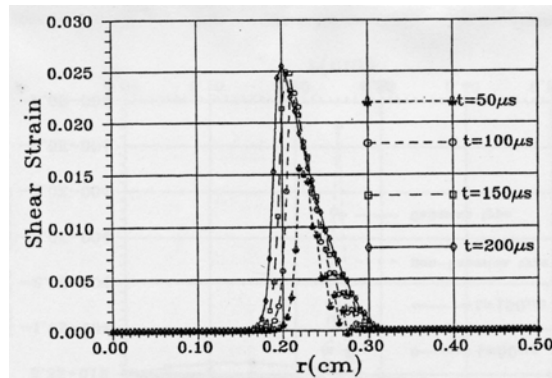


**Figure 6:** Transient average shear strain distributions vs the radial coordinate for the non-Gaussian type of laser beam with  $E_j=10J$  at different times.

### *Prediction of Reverse Plugging*

The theory of one-dimensional Euler column can be used to predict the critical laser intensity at which the reverse plugging may take place. In the laser-irradiated region, the compressive stress can be obtained as,

$$\sigma_r = -\frac{1}{2}\alpha_0 E \frac{I_{\max}(1-R_0)}{\rho C_p h} \left[ \frac{1}{\alpha}(1-e^{-\alpha t}) - \frac{1}{\alpha+\beta}(1-e^{-(\alpha+\beta)t}) \right] \quad (3)$$

where  $\alpha_0, E, \rho, C_p$  and  $R_0$  are, respectively, thermal expansion, Young's modulus, mass density, specific heat.

It is well known that the critical classical buckling stress  $\sigma_c$  of a clamped-clamped wide plate is,

$$\sigma_c = \frac{\pi^2}{12} \frac{E}{1-\nu^2} \left(\frac{h}{a}\right)^2 \quad (4)$$

The thermal stress  $\sigma_{\text{ther}} = -\sigma_{\text{rr}}$  must exceed  $\sigma_c$  if the foil in the laser-irradiated region is to buckle away from the remained region. The nondimensional “loading parameter” is  $\sigma_{\text{ther}}/\sigma_c$  and it is shown in figure 7 for different laser intensities. It is very interesting that the loading parameter is larger than one with  $I_{\text{max}} \geq 0.61\text{W}/\text{cm}^2$ . It is the critical laser intensity at which the reverse plugging takes place.

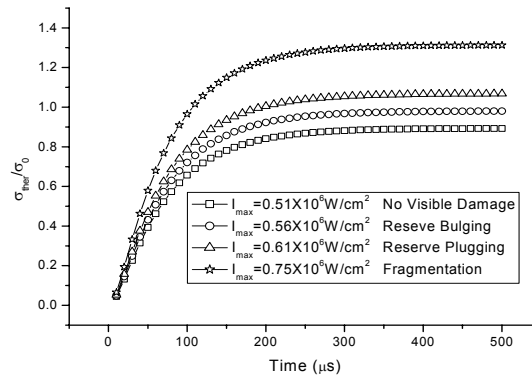


**Figure 7:** Histories of “loading parameter”

## CONCLUSIONS

A new failure mode is observed in circular brass foils induced by laser beam. The failure process consists of three stages; i.e., thermal bulging, localized shear deformation and perforation by plugging. The word ‘reverse’ in ‘reverse bulging and plugging mode’ means that bulging and plugging occur in the reverse direction of laser beam incidence. The new failure mode is analyzed with the thermal-elastic plate theory, parabolic shear deformation theory as well as one-dimensional buckling theory. The theoretical study can explain the new phenomenon and predict the critical laser intensity. The calculated results for temperature fields, deflection as well as shear deformation distribution show that the newly discovered failure mode is attributed to the spatial structure effect of laser beam.

## ACKNOWLEDGEMENTS

Support for this research program was provided partly by the NNSF of China.

## REFERENCES

1. Zhou, Y. C. and Duan, Z. P. (1998) *Int. J. Non-Linear Mech.* 33, 433.
2. Eliezer, S., Gilath, I. and Bar-Noy, T. (1990) *J. Appl. Phys.* 67, 715.